Rapidly Quenched $Ni_{45}Fe_5Mn_{40}Sn_{10}$ Heusler Alloys

Shashank Shekhar Mishra[a], Thakur Prasad Yadava[a]*, Semanti Mukhopadhyay[b],

Ram Manohar Yadav[c,d], Vajapeyajula Srinivasa Subrahmanyam[a], Nilay Krishna Mukhopadhyay[e],

Onkar Nath Srivastava[a]

[a]*Hydrogen Energy Centre, Department of Physics, Banaras Hindu University, Varanasi-221005, India*
[b]*Department of Materials Science and Engineering, Indian Institute of Technology Kanpur, Kanpur-208016, India*
[c]*Department of Materials Science and NanoEngineering, Rice University, Houston-77005, USA*
[d]*Department of Physics, Vikramajeet Singh Sanatan Dharma, College, Kanpur-208002, India*
[e]*Department of Metallurgical Engineering, Indian Institute of Technology, Banaras Hindu University, Varanasi-221 005, India*

The present work describes the synthesis and characterization of $Ni_{45}Fe_5Mn_{40}Sn_{10}$ Heusler alloys. The constituent pure metals were melted in radio frequency induction furnace to form the alloy and then cooled it quickly. The as-cast alloy was annealed at 850 °C for 24 h in vacuum and cooled in two different conditions i.e. self-cooling at room temperature in air and sudden cooling at liquid nitrogen temperature (quenched). The X-ray diffraction, scanning and transmission electron microscopic techniques have been used for structural/microstructural characterization as well as chemical analysis of the material. The effect of annealing and subsequent cooling in two different conditions has been described and discussed in the context of evolution of B2 and orthorhombic martensite with lattice parameter a= 0.65 nm, b=0.59 nm and c=0.56 nm.

Keywords: *Heusler alloys, $Ni_{45}Fe_5Mn_{40}Sn_{10}$, microstructural characterization, rapid solidification*

1. Introduction

With greater attention being placed on the sustainability of development of materials in recent times, the focus is on developing smart structures, which can combine contemporary materials science with information technology. A typical smart system comprises of a manifestation of functional materials that can offer performance in multiple dimensions. To this class of materials belong the Heusler alloys, which provide an attractive area of research due to their ferromagnetic and martensitic phase transformations because of which they exhibit multiferroic behavior. Since their discovery in 1903, when Heusler[1] reported an unexpectedly high degree of ferromagnetism in alloys comprising of an s-p element added to the Cu-Mn system, the Heusler alloys became important. After years of experimentation, it was found that a typical Heusler compound has a face centered cubic (FCC) structure which comprises, essentially, of an ordered combination of two binary B2 compounds, XY and XZ, forming the $L2_1$ structure, (Figure 1a). Both compounds are derived from the CsCl type crystal structure. It appears that the ability of compounds to form B2 structure can be correlated with their ability to form new Heusler alloys. Alloys with a structure essentially similar to the Heusler alloys that consist of an unoccupied sublattice (out of the four present) have also been discovered ($C1_b$ structure). These classes of compounds are often referred to as half- or semi- Heusler

alloys (Figure 1b). Extensive experimentation has confirmed that most of the Heusler compounds order ferromagnetically in stoichiometric composition[2,3].

Heusler alloys have attracted attention for many decades due to their different interesting physical properties. They exhibit ferromagnetic and shape memory effect simultaneously, have been given more importance due to their potential application for making devices. A class of such alloys with general formula X_2YZ (X = Ni, Co;Y= Mn;Z = Sn, Ga, In) has become a subject of intense study because of the effects like magnetic shape memory, magnetocaloric properties, half-metallic behavior and exchange bias[4-7]. The NiMnGa alloy exhibits magnetic field induced strain recovery by the mechanism of martensite variant reorientation and best-known ferromagnetic shape memory alloy[8]. Crystallographic structure of these alloys can be constructed from an arrangement of four interpenetrating FCC sub-lattices, shifted towards body diagonal and the chemical disorder within these sub-lattices causes drastic changes in the physical properties[9]. These alloys are known to exhibit first order diffusionless-phase transformations[10]. Such a phase transformation involves an abrupt change in physical properties including the lattice parameters[11]. Properties of the material that are heavily influenced by such changes, including the magnetization, may be assumed to give rise to diverse properties, in general, and electromagnetic properties, in particular, for different phases[12,13]. The effect of Co doping on the magnetic entropy
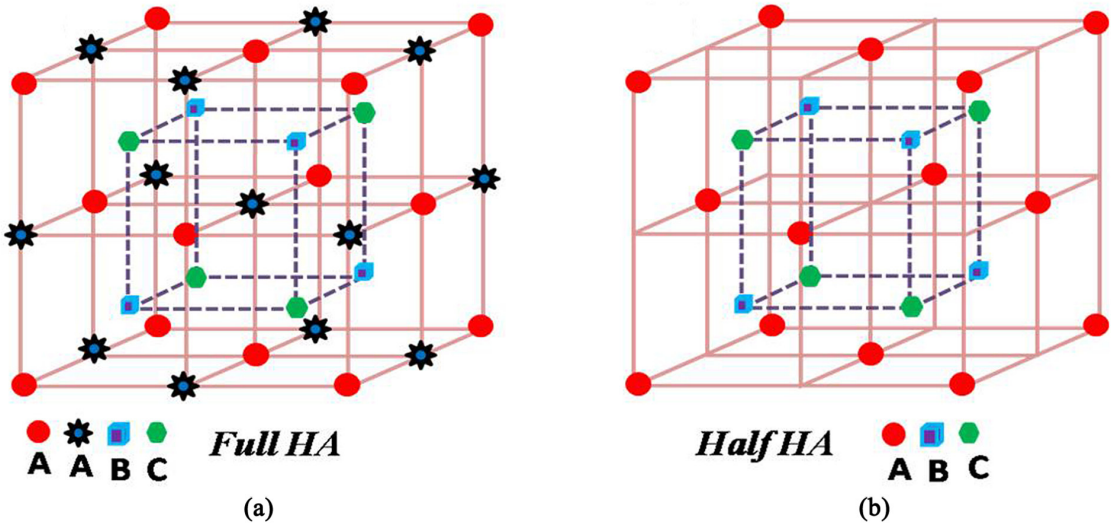
Figure 1. (a,b) Schematic crystal structures full-Heusler and half- Heusler alloys. The lattice is consisted of 4 interpenetrating f.c.c. lattices. In the case of the half-Heusler alloys (XYZ) one of the four sublattices is vacant. If all atoms were identical, the lattice would be simply the bcc.

changes in $Ni_{44-x}Fe_xMn_{45}Sn_{11}$ alloys has been studied and a martensitic phase transformation was observed with Co addition[14]. It has been reported that the NiCoMnSn shows a strongly ferromagnetic austenite phase and a non-ferromagnetic martensite phase[15,16]. The transformation-induced strains with and without applied magnetic field and magnetostriction loops at different temperatures have been measured for polycrystalline ferromagnetic and metamagnetic NiMnGa, Ni Fe(Co)Ga and NiMnSn shape memory Heusler alloys[17]. A magnetic field oriented growth of martensitic variants during the martensitic transformation in NiMnGa sample was observed, however this effect was not pronounced in the other two alloys. Such a phase transformation seems to be an interesting area of research, dedicated towards developing energy conversion and storage devices.

The present work deals with the synthesis of $Ni_{45}Fe_5Mn_{40}Sn_{10}$ Heusler alloys and their structural and microstructural characterization. The effect of slow and rapid cooling of the annealed sample in context of phase evolution has been addressed.

2. Experimental Details

All the metallic ingredients used in this study are commercially available. High purity Ni (99.99%), Fe(99.99%) and Mn (99.98%) were obtained from Sigma Aldrich and Sn (99.96%) from Alfa Aesar. Alloy ingot of $Ni_{45}Fe_5Mn_{40}Sn_{10}$ (this is known optimum composition) was prepared by radio frequency induction melting of the constituent elements corresponding to the requisite stoichiometric mixture in a silica tube under argon atmosphere. Water was flown in the outer jacket of the melting system to avoid the interaction of the melt with Si and SiO_2 (quartz) tube. The ingot was melted several times to ensure homogeneous mixing. The ingots were annealed for 24 hours in vacuum at 850°C and the as-annealed samples were then allowed to cool down under two different conditions: (i) samples were rapidly quenched

(RQ) into liquid nitrogen and (ii) samples were coolled slowly by furnace cooling. The structural characterization was carried out by X-ray diffraction in reflection mode using the X'Pert PRO PANanalytical diffractometer equipped with graphite monochromator with CuKα radiation (λ= 0.15402 nm) in the Bragg-Brentano configuration. The device was operated at the voltage and current of 40 kV and 40 mA respectively. The diffraction parameters, scan step time (in seconds) and step size (2θ°), were taken as 1.500 and 0.0200 respectively. The structural morphology of all the samples were analyzed using scanning electron microscopy (SEM) (FEI: QUANTA 200) operated at 25 kV. Detailed microstrutural investigation was performed through transmission electron microscopy (TEM) in a FEI: TECNAI-20G² equipped with single tilt sample stage, operated at 200KV. The chemical composition analysis was done by energy dispersive X-ray (EDX) analysis attached to the TEM.

3. Results and Discussion

Figure 2a shows the XRD pattern of as-cast $Ni_{45}Fe_5Mn_{40}Sn_{10}$ alloy which confirms the presence of only single phase of FCC structure with a lattice parameter: a=0.608 nm. Figure 2b, c shows the XRD patterns of $Ni_{45}Fe_5Mn_{40}Sn_{10}$ alloys annealed for 24 hours in vacuum at 850 °C and cooled down under two different conditions *i.e.* cooled in air and RQ in liquid nitrogen. The presence of a maximum intensity peak of (220) along with the other peaks in the XRD pattern reveals that the crystal structure of these two annealed alloys broadening are nearly similar to that of as-cast alloy. The annealed alloys exihibited extra peaks (marked by arrow) this suggests the appearance of another peak on annealing. However, the intensity of (200) peak in the annealed alloys is more prominent compared to the as-cast alloy. When compared with the XRD results of other NiMn-based alloys[18], it showed that the $Ni_{45}Fe_5Mn_{40}Sn_{10}$ alloy undergoes a transformation from the FCC parent phase to the
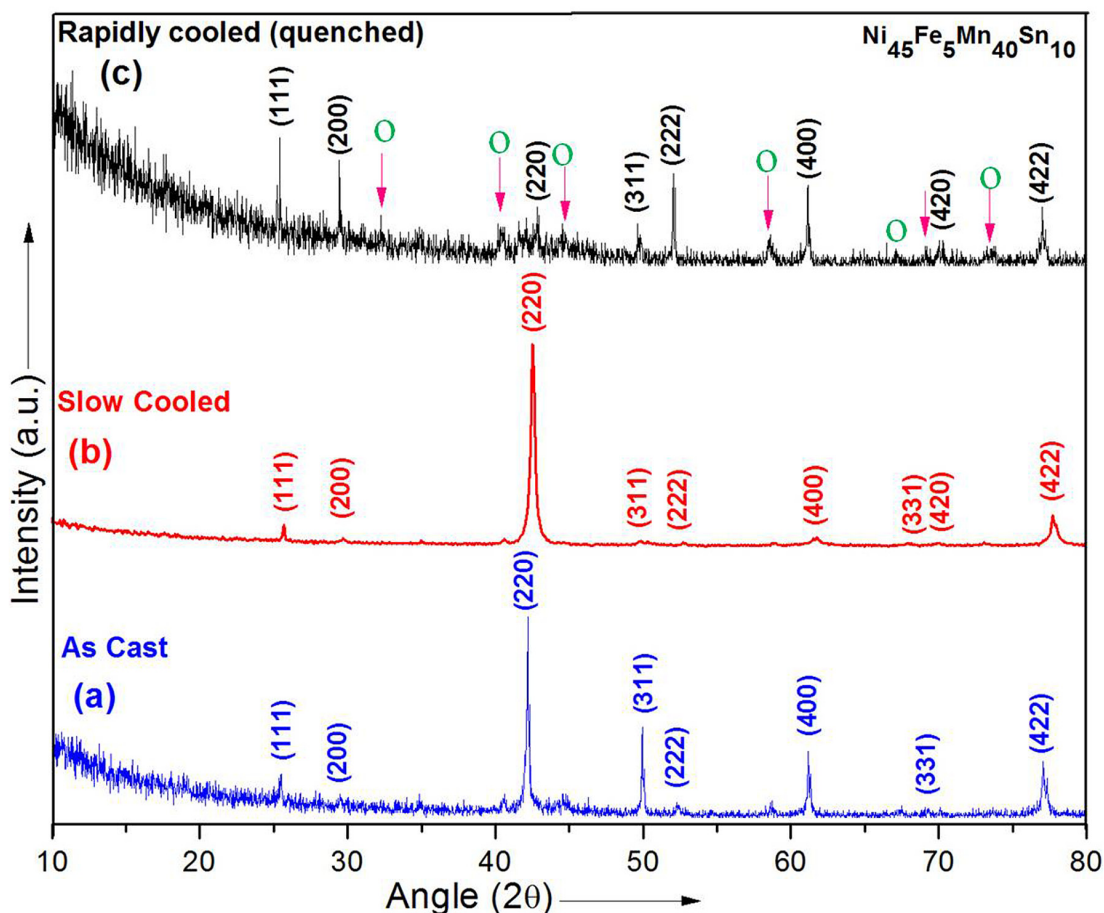
Figure 2. (a) XRD pattern of as-cast Ni$_{45}$Fe$_5$Mn$_{40}$Sn$_{10}$ alloy, (b-c) XRD patterns alloys annealed for 24 hours in vacuum at 850 °C followed by furnace cooling and rapid cooling in liquid nitrogen respectively.

orthorhombic martensite with lattice parameter a= 0.65 nm, b=0.59 nm and c=0.56 nm (Figure 2b, c).

The SEM micrographs of Ni$_{45}$Fe$_5$Mn$_{40}$Sn$_{10}$ alloys are shown in Figure 3. The as-cast alloy (Figure 3a) exhibits a typical martensite microstructure, consisting of self-accommodating martensite plates, which is also present in the annealed and subsequently furnace-cooled alloys (Figure 3b). It is clear that two morphologies: one with a bright contrast and the other one with a grey contrast, indicate that composition segregation exists in the as cast alloy. However, in the as annealed and subsequently the furnace-cooled sample, as shown in Figure 3b, the difference of contrast caused by segregation is not observed. Instead, the grey strips with different sizes are identified as the martensite plates with different orientations. The SEM image depicted in Figure 3c shows the effect of annealing and subsequent RQ treatment on microstructure, the homogeneous grains with sharp grain boundary are observed and it is clear that the chemical homogeneity is greatly improved in the annealed and subsequently RQ alloy.

Further characterization of the as-cast as well as annealed samples was carried out through TEM. Figure 4 shows the TEM microstructure and the corresponding selected area diffraction (SAD) pattern of the Ni$_{45}$Fe$_5$Mn$_{40}$Sn$_{10}$ alloys *i.e.* as-cast in Figure 4a, b, furnace cooled Figure 4c, d and annealed subsequently RQ Figure 4e, f alloys, respectively. All the micrographs Figure 4a, c, d, show submicron sized grains in the range of 100-200 nm. A significant microstructural variation has been observed in annealed and subsequently RQ Figure 4d. The SAD pattern analysis of the alloys confirms the formation of FCC Heusler phase, however both the annealed alloys show the polycrystalline ring pattern Figure 4d, f. This result is consistent with the XRD result, which also reveals the formation of FCC phases with lattice parameter a=0.608 nm. For the composition determination, a quantitative Energy dispersive X-ray analysis (EDX) linked with TEM was performed. Figure 5a, b present EDX spectra of the Ni$_{45}$Fe$_5$Mn$_{40}$Sn$_{10}$ annealed and subsequently RQ alloy from region A and B of Figure 4e respectively. Based on the EDX quantitative analysis, the compositions of the alloys (in at %) have been found to be Ni$_{45.2}$Fe$_{4.8}$Mn$_{39.6}$Sn$_{10.4}$, which are in close agreement to the stoichiometric proportions of nominal compositions. Within the limit of delectability of EDX, no discernible evidence of oxygen was detected in the annealed alloy.

(a)   (b)   (c)
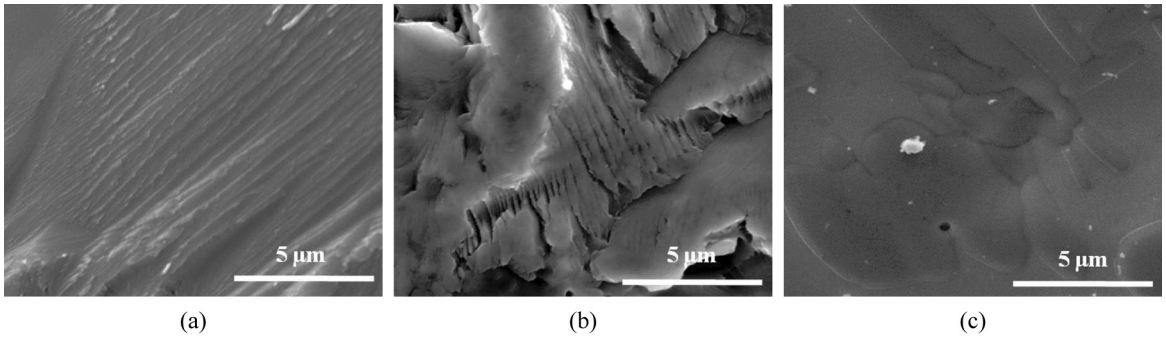
Figure 3. SEM micrograph of (a) as cast, (b) annealed & subsequently furnace cooled and (c) annealed & subsequently rapidly cooled $Ni_{45}Fe_5Mn_{40}Sn_{10}$ alloys.

(a)   (b)   (c)

(d)   (e)   (f)
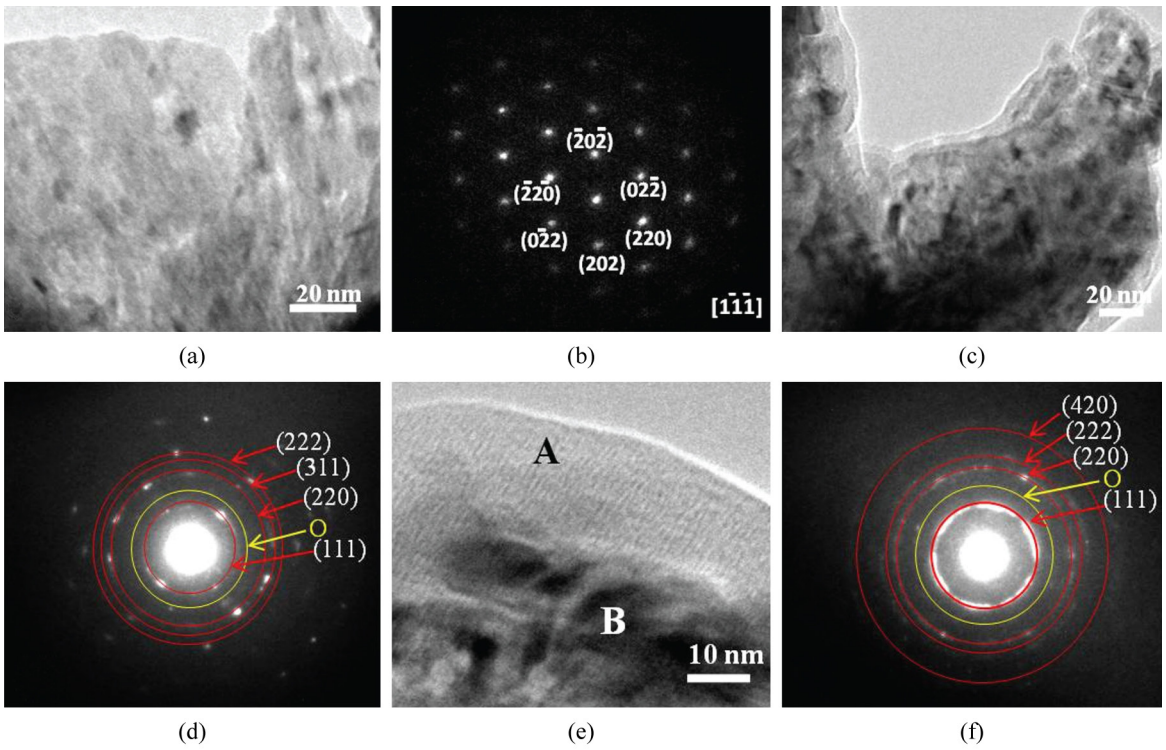
Figure 4. TEM microstructure and the corresponding selected area diffraction (SAD) pattern of the $Ni_{45}Fe_5Mn_{40}Sn_{10}$ alloys *i.e.* as-cast (a-b), annealed and subsequent furnace cooled Figure 4c, d and annealed and subsequent rapidly cooled (e-f) alloys respectively.

(a)   (b)
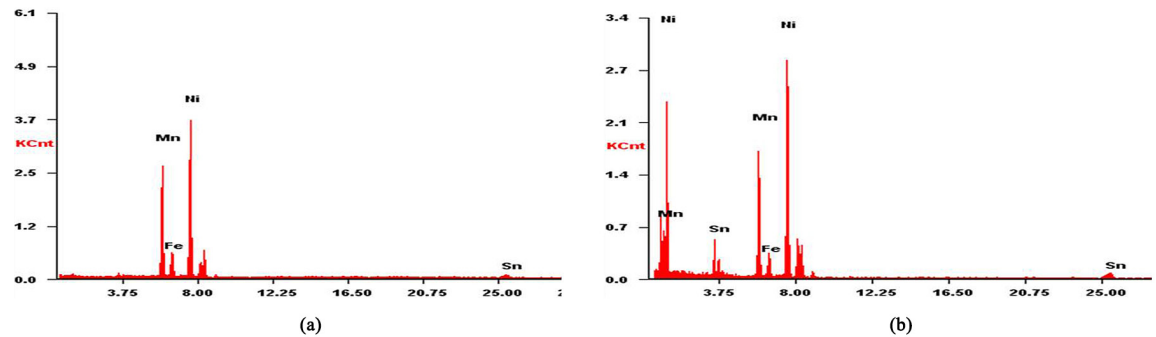
Figure 5. (a and b) Energy dispersive spectra of the annealed and subsequently RQ alloy from region A and B of Figure 4e respectively.

4. Conclusions

Single phase Ni$_{45}$Fe$_5$Mn$_{40}$Sn$_{10}$ Heusler alloy was synthesized using radio frequency induction melting technique. The reductions in the grain sizes compared to that of the bulk counterpart were observed in the annealed and subsequently RQ alloys. In the as-cast sample, micron size grains were found while in the annealed and subsequently RQ alloy, submicron size grains with high-density grain boundaries areas were observed which are orthorhombic martensite with lattice parameter a= 0.65 nm, b=0.59 nm and c=0.56 nm.

References

1. Heusler F. Über magnetische Manganlegierungen. *Deutsche Physikalische Gesellschaft*. 1903; 12:219.

2. Potter HH. The X-ray structure and magnetic properties of single crystals of Heusler alloy. *Proceedings of the Physical Society*. 1929; 41:135.

3. Bradley AJ and Rodgers JW. The crystal structure of the heusler alloys. *Proceedings of the Royal Society of London. Series A, Mathematical and Physical Sciences*. 1934; 144(852):340-359. http://dx.doi.org/10.1098/rspa.1934.0053.

4. Kainuma R, Imano Y, Ito W, Sutou Y, Morito H, Okamoto S, et al. Magnetic-field-induced shape recovery by reverse phase transformation. *Nature*. 2006; 439(7079):957-960. http://dx.doi.org/10.1038/nature04493. PMid:16495995.

5. Krenke T, Duman E, Acet M, Wassermann EF, Moya X, Manosa L, et al. Inverse magnetocaloric effect in ferromagnetic Ni-Mn-Sn alloys. *Nature Materials*. 2005; 4(6):450-454. http://dx.doi.org/10.1038/nmat1395. PMid:15895096.

6. Sakuraba Y, Hattori M, Oogane M, Ando Y, Kato H, Sakuma A, et al. Giant tunneling magnetoresistance in Co$_2$MnSi/Al–O/Co$_2$MnSi magnetic tunnel junctions. *Applied Physics Letters*. 2006; 88(19):192508. http://dx.doi.org/10.1063/1.2202724.

7. Wang BM, Liu Y, Ren P, Xia B, Ruan KB, Yi JB, et al. Large exchange bias after zero-field cooling from an unmagnetized state. *Physical Review Letters*. 2011; 106(7):077203. http://dx.doi.org/10.1103/PhysRevLett.106.077203. PMid:21405539.

8. Wuttig M, Liu L, Tsuchiya K and James RD. Occurrence of ferromagnetic shape memory alloys (invited). *Journal of Applied Physics*. 2000; 87(9):4707-4711. http://dx.doi.org/10.1063/1.373135.

9. Brown PJ, Kanomata T, Neumann K, Neumann KU, Ouladdiaf B, Sheikh A, et al. Atomic and magnetic order in the shape memory alloy Mn$_2$NiGa. *Journal of Physics Condensed Matter*. 2010; 22(50):506001. http://dx.doi.org/10.1088/0953-8984/22/50/506001. PMid:21406811.

10. Bhattacharya K and James RD. Applied physics. The material is the machine. *Science*. 2005; 307(5706):53-54. http://dx.doi.org/10.1126/science.1100892. PMid:15637259.

11. Spaldin NA and Fiebig M. The renaissance of magnetoelectric multiferroics. *Science*. 2005; 309(5733):391-392. http://dx.doi.org/10.1126/science.1113357. PMid:16020720.

12. Ramesh R and Spaldin NA. Multiferroics: progress and prospects in thin films. *Nature Materials*. 2007; 6(1):21-29. http://dx.doi.org/10.1038/nmat1805. PMid:17199122.

13. James RD and Zhang Z. The interplay of magnetism and structure in functional materials. *Springer Series in Materials Science*. 2005; 79(1):159-175.

14. Liu HS, Zhang CL, Han ZD, Xuan HC, Wang DH and Du YW. The effect of Co doping on the magnetic entropy changes in Ni$_{44-x}$Co$_x$Mn$_{45}$Sn$_{11}$ alloys. *Journal of Alloys and Compounds*. 2009; 467(1-2):27-30. http://dx.doi.org/10.1016/j.jallcom.2007.11.137.

15. Srivastava V, Chen X, James R D. Hysteresis and unusual magnetic properties in the singular Heusler alloy. *Applied Physics Letters*. 2010;97(1):014101-014103.

16. Srivastava V, Song Y, Bhatti K and James RD. The direct conversion of heat to electricity using multiferroic alloys. *Advanced Energy Materials*. 2011; 1(1):97-104. http://dx.doi.org/10.1002/aenm.201000048.

17. Chernenko VA, Barandiarán JM, L'vov VA, Gutiérrez J, Lázpita P, Orue I. Temperature dependent magnetostrains in polycrystalline magnetic shape memory Heusler alloys. *Journal of Alloys and Compounds*. 2013; 577(Suppl 1):S305-S308.

18. Song Y, Chen X, Dabade V, Shield TW and James RD. Enhanced reversibility and unusual microstructure of a phase-transforming material. *Nature*. 2013; 502(7469):85-88. http://dx.doi.org/10.1038/nature12532. PMid:24091977.